Carbohydrate Polymers 103 (2014) 170–178

Contents lists available at ScienceDirect

Carbohydrate Polymers

journal homepage: www.elsevier.com/locate/carbpol

Enhanced osteogenic differentiation of MC3T3-E1 on rhBMP-2-immobilized titanium via click reaction

Eun-Cheol Kim [a], Tae-Hee Kim [b], Jae-Hoon Jung [b], Sung Ok Hong [b], Deok-Won Lee [a,b,*]

[a] Department of Maxillofacial Tissue Regeneration and Research Center for Tooth & Periodontal Regeneration (MRC), School of Dentistry, Kyung Hee University, 1 Heogi-dong, Dongdaemun-gu, Seoul 130-701, Republic of Korea
[b] Department of Oral and Maxillofacial Surgery, Kyung Hee University Dental Hospital at Gangdong, Kyung Hee University, Seoul 134-727, Republic of Korea

ARTICLE INFO

Article history:
Received 14 August 2013
Received in revised form 4 November 2013
Accepted 9 December 2013
Available online 16 December 2013

Keywords:
Titanium surface
BMP-2
MC3T3-E1 cell
Osteogenic differentiation

ABSTRACT

In the present study, we report about the efficacy of titanium surface-immobilized with bone morphogenetic protein-2 (BMP-2) via click reaction on enhanced osteogenic differentiation of MC3T3-E1 cells. The surface was characterized by static contact angles and XPS measurements, which indicated that pristine titanium (Ti-1) was successfully surface-modified via click chemistry (aminated titanium, Ti-4). By quantitative analysis of heparin immobilized on aminated titanium (Ti-4), we found that the Ti-4 can be used as a good candidate to immobilize biomolecules such as heparin. BMP-2 from titanium immobilized with BMP-2 (Ti-6) was released for a period of 28 days in a sustained manner. The highest proliferation rate of MC3T3-E1 cells was observed on Ti-6. Through in vitro tests including alkaline phosphatase (ALP) activity, calcium deposition and real-time polymerase chain reaction (real-time PCR), we found that Ti-6 can be used as a good implant to enhance the osteogenic differentiation of MC3T3-E1 cells.

1. Introduction

The surface properties of materials contacting with biological systems play significant roles in determining the outcome at the interface between them (Mager, LaPointe, & Stevens, 2011; Prime & Whitesides, 1991). In dental and orthopedic surgeries, the surfaces of implant materials are often modified to improve the rates of osseointegration and biomechanical fixation.

Titanium (Ti) and titanium alloy have been widely used in hard tissue replacement as well as cardiac and cardiovascular applications (Liu, Chu, & Ding, 2004). There have been numerous reports about surface modification methods for the enhanced osteogenic activity of these materials; mechanical methods (Buser et al., 1999; Sutherland, Forshaw, Allen, Brown, & Williams, 1993; Wennerberg, Albrektsson, Johansson, & Andersson, 1996) including machining, grinding, polishing and blasting as well as chemical methods, such as acid-etching, H_2O_2-etching, alkali-etching, sol–gel coating, anodic oxidation, chemical vapor deposition and biochemical modification have been studied to enhance the osteogenic activity (Andreazza, De Barros, Andreazza-Vignolle, Rats, & Vandenbulcke, 1998; Domenichini et al., 1999; Hua, Shi, Zhang, Ruan, & Zhao, 2001; Kapoor, Bhaumik, Inagaki, Kuraoka, & Yazawa, 2002; Lee, Kim, Kim, Choi, & Lee, 2004; Xiao, Textor, & Spencer, 1998; Xue, Deng, Lai, & Chen, 1998).

The formation of hydroxyl, carboxyl, amine, azide and alkyne groups on the surface of Ti can be effective ways to conjugate various biomolecules by these functional groups. Among these, click reaction, based on the reaction between azide and alkyne groups, is highly efficient due to both high conversion and selectivity under mild conditions, reactive process occurring in an aqueous medium and high yield (Kolb, Finn, & Sharpless, 2001; Rostovtsev, Green, Fokin, & Sharpless, 2002), as compared to another reactions such as amide reaction, disulfide reaction, silylanization and polydopamination. Moreover, click reaction has been developed as a versatile method for conjugating a variety of organic, polymeric and biological molecules (van Dijk, Rijkers, Liskamp, van Nostrum, & Hennink, 2009).

To examine the feasibility of aminated Ti surface via click reaction for immobilizing biological molecules, heparin was surface-immobilized, followed by immobilization of recombinant human bone morphogenetic protein-2 (rhBMP-2) via physical interaction with heparin (Ruppert, Hoffmann, & Sebald, 1996). rhBMP-2, an effective growth factor, plays a significant role in the formations of bone and cartilage.

In the present study, we designed and prepared aminated Ti (Ti-**4**), which was conjugated via click reaction between the azide group of 2-azidoethanamine and the propargyl group of propargylated Ti (Ti-**3**). Heparin was conjugated to Ti-**4** via amide bond by condensation reaction (heparinized Ti, Ti-**5**), followed by

* Corresponding author at: Department of Oral and Maxillofacial Surgery, Kyung Hee University Dental Hospital at Gangdong, #892 Dongnam-ro, Gangdong-gu, Seoul 134-727, Republic of Korea. Tel.: +82 2 440 6172; fax: +82 2 440 7525.
E-mail addresses: verycutebear@hanmail.net, verycutebear@khu.ac.kr (D.-W. Lee).

0144-8617/$ – see front matter © 2013 Elsevier Ltd. All rights reserved.
http://dx.doi.org/10.1016/j.carbpol.2013.12.023

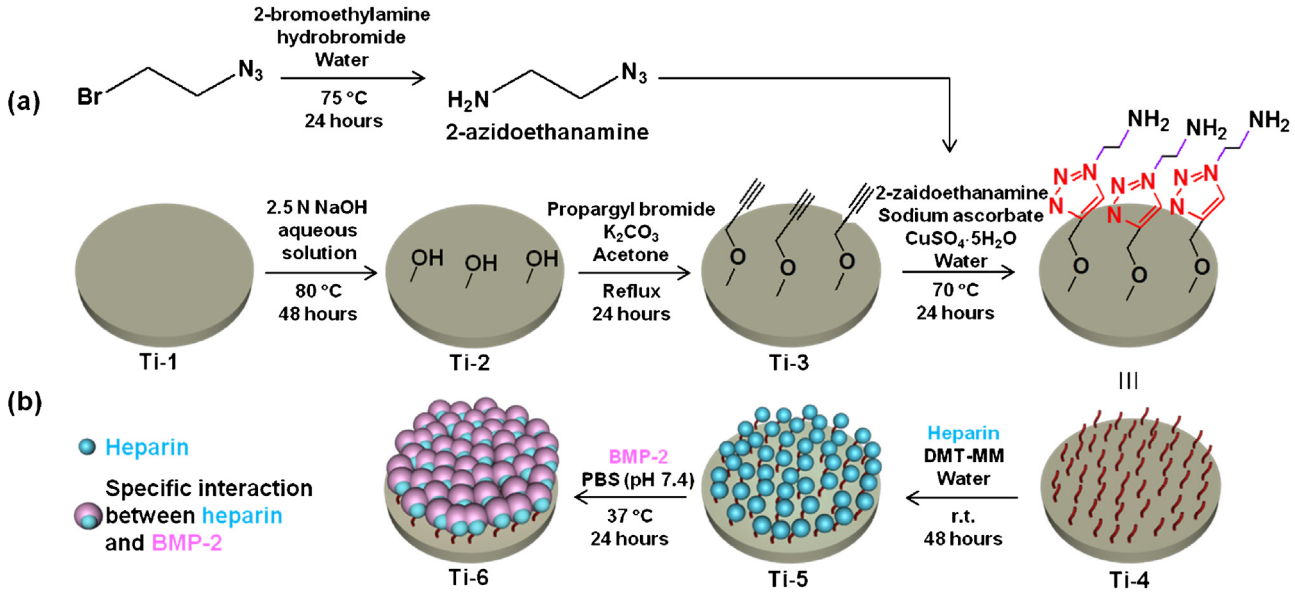

Fig. 1. (A) Synthetic route of 2-azidoethanamine and (B) schematic illustration of preparing Ti-**1**–**6**.

immobilization of rhBMP-2 onto Ti-**5** (rhBMP-2-immobilized Ti, Ti-**6**). In vitro tests, including MC3T3 cell proliferation, alkaline phosphatase (ALP) activity, calcium deposition and bone-related mRNA gene expressions, were carried out.

2. Materials and methods

2.1. Materials

Titanium dioxide disks (Ti-**1**, diameter: 10 mm, height: 3 mm) were kindly obtained from DIO Co. (Busan, Republic of Korea). Propargyl bromide, potassium carbonate (K_2CO_3), sodium ascorbate and copper (II) sulphate pentahydrate ($CuSO_4 \cdot 5H_2O$) were supplied from Sigma–Aldrich (St. Louis, MO, USA). Heparin sodium (molecular weight: 12,000–15,000 g/mol) was purchased from Acrose Organics (NJ, USA). rhBMP-2 was purchased from Peprotech (NJ, USA). Fetal bovine serum (FBS), penicillin–streptomycin (PS) and phosphate buffered saline (×1 PBS, pH 7.4) were supplied from Gibco BRL (Gaithersburg, MD). (4-(4,6-dimethoxy-1,3,5-triazin-2-yl)-4-methylmorpholinium chloride) (DMT-MM) was purchased from Wako (Osaka, Japan). All organic solvents were used as received without further purification.

2.2. Surface propargylation (Ti-**3**)

Ti-**1** was treated using 2.5 N NaOH aqueous solution (500 mL) at 80 °C for 48 h. After sonicating, the surface-treated samples were washed with distilled water for 5 min three times, dried with nitrogen gas, and then stored at room temperature (Ti-**2**). Ti-**2** and K_2CO_3 (6.91 g, 0.05 mol) were mixed together in anhydrous acetone (500 mL). Propargyl bromide (4.31 mL, 0.05 mol) was added to this mixture at room temperature and refluxed for 24 h to induce click reaction. After taking out the samples, they were repeatedly washed with acetone and distilled water three times, dried with nitrogen gas, and then stored at room temperature (Ti-**3**) (Fig. 1).

2.3. Surface heparinization (Ti-**6**)

Ti-**3** and 2-azidoethanamine (1.41 g, 0.02 mol) were mixed in distilled water (50 mL). Sodium ascorbate (3.96 g, 0.02 mol) and $CuSO_4 \cdot 5H_2O$ (0.89 g, 3.57 mmol) were added to this mixture at room temperature and reacted at 70 °C for 24 h. After washing with distilled water three times, the samples were dried with nitrogen gas, and then stored at room temperature (Ti-**4**). In order to escape the immobilization of heparin at the one-side and the circumference of Ti-**4**, the points were scrubbed with sandpaper. Heparin (92 mg) and DMT-MM (1 g, 3.61 mmol) were dissolved in distilled water (40 mL). This solution was continuously stirred at room temperature for 1 h, and then Ti-**4** was added. The mixture was reacted at room temperature for 48 h to induce amide bond by condensation reaction. After washing the samples with distilled water three times, they were dried with nitrogen gas, and then stored at −20 °C (Ti-**5**) prior to use. Ti-**5** and rhBMP-2 (10 ng) were mixed in PBS (1 mL, pH 7.4) and incubated at 37 °C for 24 h with orbital agitation at 80 rpm. After washing the samples with PBS three times, they were dried with nitrogen gas. Prior to use, they were stored in a freezer (−20 °C) (Ti-**6**) (Fig. 1).

2.4. Scanning electron microscope observation

The surface morphologies of Ti-**1**–**6** were observed by scanning electron microscopy (SEM, S-2300, Hitachi, Japan). First, Ti-**1**–**6** fixed on metal mounts were gold-coated by a sputter-coater (Eiko IB, Japan) with an accelerating voltage of 15 kV, and then observed at a magnification of ×1.5k.

2.5. Static contact angles measurement

Static contact angles measurement was carried out using a sessile drop method at 20 °C with 3 μL of distilled water droplet under a relative humidity of 60%, in advance adjusted to 71.8 mN/m of surface tension, as measured by a telescopic goniometer (Pheonix 300, Seoul, Republic of Korea).

2.6. Surface chemical compositions measurement

The surface chemical compositions of Ti-**1**–**6** were examined by X-ray photoelectron spectroscopy (XPS) measurement. XPS measurement was carried out using a Thermo Electron (U.K) unit under a grazing angle of 90° and in a high vacuum (less than 3.1×10^{-9} Torr). A monochromatic aluminum Kα X-ray radiation source (photoelectron energy = 1486.6 eV) was used. Wide scanned

XPS was obtained at a pass of 187.7 eV and measured from 0 to 1400 eV.

2.7. Quantitative analysis of heparin

Quantitative analysis of heparin immobilized on Ti-**5** was carried out using toluidine blue method (Kim et al., 2011). Briefly, 500 μL toluidine blue solution (0.005%) was added to a mixture of Ti-**5** in 2 mL aqueous NaCl solution (0.2%). After gentle shaking for 30 min, hexane (3 mL) was added. The Ti-**5** was removed from the solution, and then the absorbance of the aqueous layer was measured at a wavelength of 620 nm. The quantitative amount of heparin was calculated using a calibration curve determined from known concentrations of heparin. The calibration curve was prepared using seven concentrations of heparin (0.1, 0.5, 2, 3, 4, 5 and 10 μg/mL) in aqueous NaCl solution.

2.8. Practical immobilizing amount of rhBMP-2 on Ti-**6**

A fixed amount of rhBMP-2 (10 ng) was immobilized on Ti-**5** as mentioned in Section 2.3. After the immobilizing process, 100 μg of the remaining solution was analyzed by a microplate reader (Bio-Rad, Hercules, CA, USA) using an enzyme-linked immunosorbent assay (ELISA) (Mundy et al., 1999) to examine free rhBMP-2. The practical amount of rhBMP-2 immobilized was calculated by the comparison with standard curve obtained from several concentration of rhBMP-2. Optical density was measured at 495 nm.

2.9. Release kinetics of rhBMP-2 from Ti-**6**

Ti-**6** was added to a vial filled with 3 mL PBS (pH 7.4) and then incubated at 37 °C at 100 rpm. At each predetermined time point (1, 2, and 8 h, 1, 3, 5, 7, 14, 21 and 28 days), 1 mL of the supernatant was collected, and then same volume of fresh PBS was added to the vial. Prior to the measurement, the collected supernatant was stored in a refrigerator (−20 °C). The release of rhBMP-2 was determined using the ELISA kit according to manufacturer's instructions mentioned in Section 2.7. Optical density of the collected supernatant was measured at 495 nm.

2.10. MC3T3-E1 cell proliferation assay

MC3T3-E1 cells (density: 5×10^3 cells/well) were seeded on Ti-**1**, **2**, **5** and **6** in a 48-well culture plate as well as control (48-well plate). 1 mL of Dulbecco's modified eagle medium (DMEM) containing 10% FBS and 1% PS was added to these cells and the plate was incubated for 1, 3 and 7 days. The medium was changed once in every three days. Nuclei and cytoskeletons of the cells cultured on all samples were stained using by 4′,6-diamidino-2-phenylindole (DAPI) and F-actin methods, as observed by fluorescence microscope (OLYMPUS DP2-BSW, NY, USA) at ×200. At each predetermined time point, each sample was rinsed with PBS (pH 7.4) and then analyzed using a cell counting kit (CCK-8). The reagent was added to the samples and carefully transferred to a 96-well culture plate after 2 h of incubation. The optical density was measured by a microplate reader at 450 nm.

2.11. Alkaline phosphatase (ALP) activity assay

MC3T3-E1 cells (a density of 5×10^3 cells/well) were seeded on Ti-**1**, **2**, **5** and **6** in a 48-well culture plate as well as control (48-well plate). Osteogenic media (DMEM containing 10% FBS, 1% PS, 10 mM β-glycero phosphate disodium salt hydrate, 300 μM ascorbic acid and 0.1 μM dexamethasone) was added to each well and the plates were incubated for 7, 14 and 21 days. At each predetermined time point, all of the cell-seeded samples were washed with PBS (pH 7.4), and then diluted in 1× RIPA buffer (50 mM Tris–HCl (pH 7.4), 150 mM NaCl, 0.25% deoxycholic acid, 1% NP-40 and 1 mM EDTA). A protease inhibitor cocktail tablet (Roche, Mannheim, Germany) was added. The cells in RIPA buffer were lysed for 20 min in ice. Each lysate was centrifuged at 4 °C for 10 min to remove the cell debris. The supernatant was then incubated with *p*-nitrophenyl phosphate (PNPP). The reaction with PNPP was terminated by adding 50 μL of 1 N NaOH. ALP activity was determined by measuring the conversion of PNPP to *p*-nitrophenol. The optical density was measured by a microplate reader at 405 nm.

Table 1
Primers of bone-related mRNA genes; OSX, Runx2, COL1, OP, OC and BSP.

Genes	Primers	
OSX	Sense	5′-TTG AGG AAG AAG CTC ACT ATG GCT CCA G-3′
	Antisense	5′-GCT GAA AGG TCA GCG TAT GGC T-3′
Runx2	Sense	5′-TCG TCA GCA TCC TAT CAG TTC CCA-3′
	Antisense	5′-CCA TCA GCG TCA ACA CCA TCA TTC TGG TTA G-3′
COL1	Sense	5′-CGT GGC GAC CAA GGT CCA GT-3′
	Antisense	5′-AGG GAG ACC CAG AAT ACC GGG AG-3′
OP	Sense	5′-TGT GTC CTC TGA AGA AAC CA-3′
	Antisense	5′-TGG CTT TCG TTG GAC TTA CT-3′
OC	Sense	5′-AGC AAA GGT GCA GCC TTT GT-3′
	Antisense	5′-GCG CCT GGG TCT CTT CAC T-3′
BSP	Sense	5′-CAG CGG CCC TGA GTC TGA CAA A-3′
	Antisense	5′-TCA CAA GCA GGG TTA AGC TCA CAC TG-3′

2.12. Calcium deposition assay

MC3T3-E1 cells (a density of 5×10^3 cells/well) were seeded on Ti-**1**, **2**, **5** and **6** as well as control (48-well plate), and then incubated for 7, 14 and 21 days. At each predetermined time point, the cell-seeded samples were washed twice with PBS (pH 7.4), fixed for 20 min using 3.7% formaldehyde and washed with PBS again. All of the samples were stained using 40 mM alizarin S-red staining solution (pH 4.2) and incubated at 37 °C under 5% CO_2 for 1 h. The staining solution was removed after 1 h, the cells were washed with distilled water three times, and then observed by confocal laser scanning microscopy (CLSM, Eclipse E600W, Nikon, Tokyo, Japan). For a quantitative analysis, the stained cells were desorbed with 10% 1-hexadecylpyridinium chloride and the absorbance was measured by a microplate reader at 540 nm.

2.13. Real-time polymerase chain reaction (real-time PCR)

The total RNA of MC3T3-E1 cells (a density of 5×10^3 cells/mL) cultured on Ti-**1**, **2**, **5** and **6** as well as control (48-well plate) for 7, 14 and 21 days were isolated using RNeasy Plus Mini Kit (Qiagen, CA, USA). According to manufacturer's instructions, 1 μg of total RNA was extracted from all samples and transcribed into cDNA with AccuPower CycleScript RT Premix (Bioneer, Daejeon, Republic of Korea). Real-time PCR amplifications on all samples were carried out by AccuPower PCR PreMix (Bioneer, Daejeon, Republic of Korea). The primers of the measured mRNA genes were as shown in Table 1: osterix (OSX) – 5′-TTG AGG AAG AAG CTC ACT ATG GCT CCA G-3′ (sense) and 5′-GCT GAA AGG TCA GCG TAT GGC T-3′ (antisense), runt-related transcription factor 2 (Runx2) – 5′-TCG TCA GCA TCC TAT CAG TTC CCA-3′ (sense) and 5′-CCA TCA GCG TCA ACA CCA TCA TTC TGG TTA G-3′, type I collagen (COL1) – 5′-CGT GGC GAC CAA GGT CCA GT-3′ (sense) and 5′-AGG GAG ACC CAG AAT ACC GGG AG-3′ (antisense), osteopontin (OP) – 5′-TGT GTC CTC TGA AGA AAC CA-3′ (sense) and 5′-TGG CTT TCG TTG GAC TTA CT-3′ (antisense), osteocalcin (OC) – 5′-AGC AAA GGT GCA GCC TTT GT-3′ (sense) and

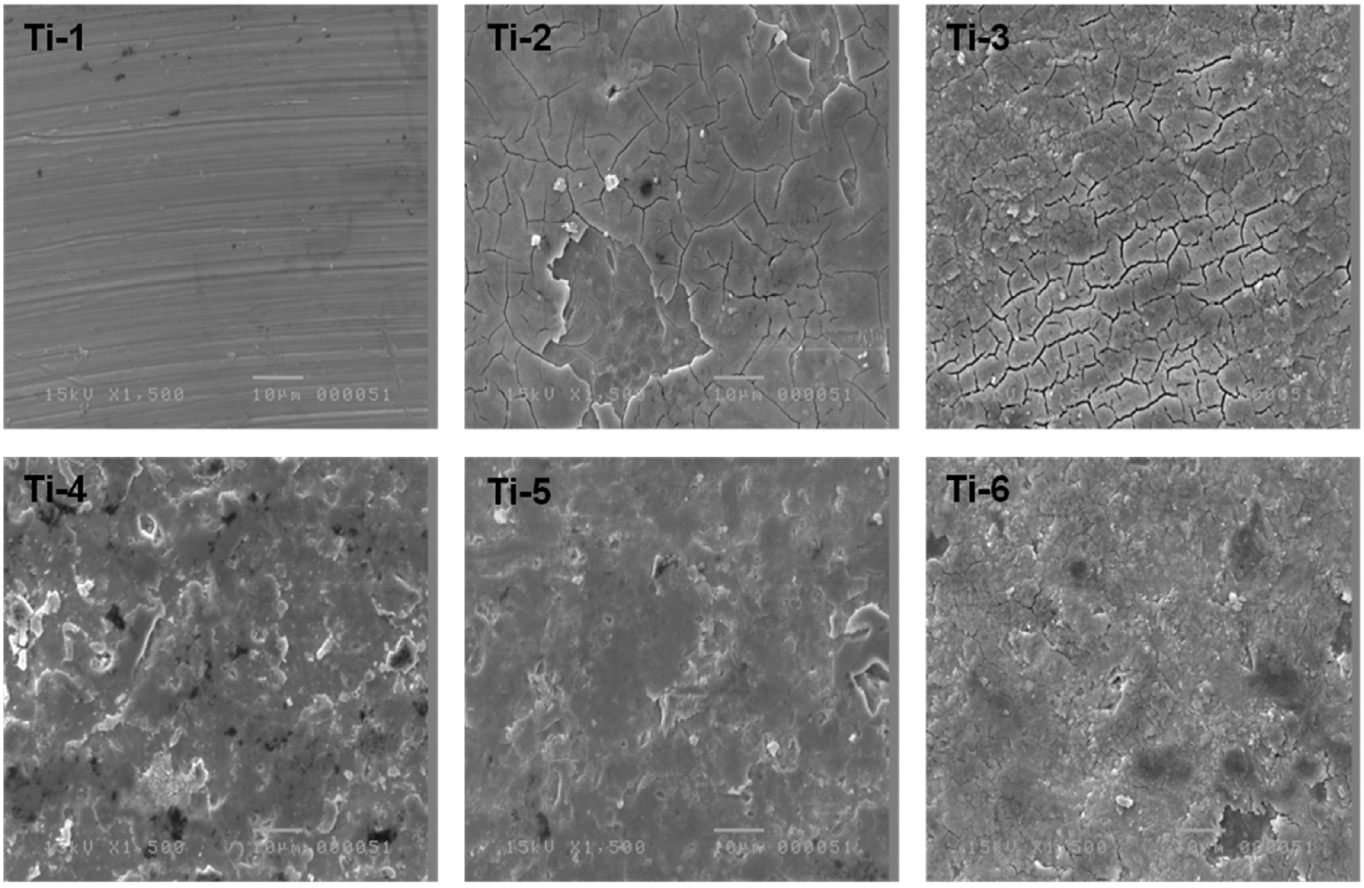

Fig. 2. SEM images of Ti-**1**–**6**, as observed at ×1500.

5′-GCG CCT GGG TCT CTT CAC T-3′ (antisense), and bone sialoprotein (BSP) – 5′-CAG CGG CCC TGA GTC TGA CAA A-3′ (sense) and 5′-TCA CAA GCA GGG TTA AGC TCA CAC TG-3′ (antisense). Real-time PCR was analyzed using iQ SYBR Green supermix (Bio-Rad, Hercules, CA, USA). Threshold cycle values were calculated by a comparative CT method. The fold change of control (48-well plate) at 7 days of culture was set at 1-fold and the ratio of the normalized fold change was then calculated. The real-time PCR amplifications were carried out under a cycle of 10 s at 95 °C, 30 s at 57–62 °C (OSX: 59 °C, Runx2: 62 °C, COL1: 60 °C, OP: 56 °C, OC: 57 °C, BSP: 61 °C) and 30 s at 72 °C for 45 cycles after the initial denaturation step for 10 min at 95 °C.

2.14. Statistical analysis

All experiments were carried out three times. Student's *t*-test was used to confirm the statistical significance of each data, as compared to control designated in each experiment. A value of $^{*}p < 0.05$ was considered statistically significant.

3. Results

3.1. Surface characterizations

Fig. 2 shows the surface morphologies of Ti-**1**–**6**, as observed by SEM. Significant differences in the surface morphologies were observed between unmodified and surface-modified samples. The smooth surface of Ti-**1** was cracked by the treatment of 2.5 NaOH. The crack still remained after the surface treatment of propargyl bromide, whereas it was disappeared on the surfaces of Ti-**4**–**6** due to the surface treatments of 2-azidoethanamine, heparin and rhBMP-2. The static contact angles of Ti-**1**–**6** were shown in Table 2. The static contact angle of Ti-**1** was 71.55°, whereas Ti-**2** showed a more hydrophilic surface (37.91°), indicating that hydroxyl groups were produced on the surface of Ti-**2**. Moreover, the static contact angles of Ti-**3**–**6** were different due to the surface modifications using different components including propargyl, 2-azidoethanamine as the linker, heparin and rhBMP-2. By wide-scanned XPS spectra measurement (Table 2), the C1s percentage of

Table 2
Changes in the S2p, C1s, N1s and O1s percentages of Ti-**1**–**6** and their static contact angles.

	C1s (283.7 eV, %)	N1s (399.2 eV, %)	O1s (528.8 eV, %)	S2p (163.8 eV, %)	Static contact angle (°)
Ti-**1**	29.21	0.32	51.27	0.25	71.55 ± 2.95
Ti-**2**	14.11	0.14	62.24	0.31	37.91 ± 2.80
Ti-**3**	32.09	0.47	52.12	0.32	64.10 ± 2.53
Ti-**4**	28.50	3.12	46.15	0.21	42.45 ± 1.75
Ti-**5**	30.05	1.28	45.04	5.89	40.80 ± 1.08
Ti-**6**	29.06	0.66	54.82	3.26	29.19 ± 2.37

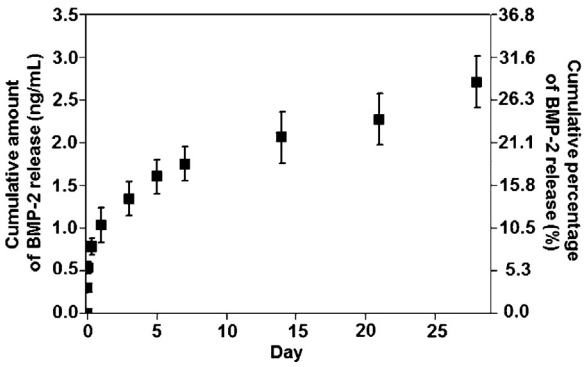

Fig. 3. Release kinetic of BMP-2 from Ti-**6** for 28 days of incubation.

Ti-**1** was 29.33%, which might be due to contamination. This fact made it difficult to quantitatively analyze the XPS spectra of Ti-**1**–**6**. However, Ti-**1** showed higher O1s percentage than Ti-**1** and **3**, which was attributed to the production of OH group. A significant increase in the N1s percentage was observed on Ti-**3** due to the existence of propargyl group. Decreased N1s percentage was observed on Ti-**4**–**6** due to the immobilization of heparin and rhBMP-2. Moreover, a significant increase in the S2p percentage was observed on Ti-**5** and **6**, mainly attributed to the immobilization of heparin. However, S2p percentage was decreased on Ti-**6** due to the immobilization of BMP-2.

3.2. Quantitative analysis of heparin

The amount of heparin immobilized on Ti-**5** was 4.1 ± 0.27 μg/sample, which was bound to the titanium surface more than 68-fold, as compared to the previous study (Kim et al., 2011). 3-Aminopropyltriethoxysilane (APTES) was surface-treated on titanium to immobilize heparin in the previous study (Shimasaki et al., 1999). On the other hand, propargyl groups were produced onto the surface of Ti-**2** in the present study. As a result, it was judged that propargyl group onto titanium surface can be used as an intermediate tool to effectively immobilize biomolecules such as heparin.

3.3. Release kinetics of rhBMP-2 from Ti-*6*

The practical amount of rhBMP-2 immobilized was 9.55 ± 0.01 ng, indicating that the loading efficiency was 99.5%. Fig. 3 shows the release kinetic of rhBMP-2 from Ti-**6** for a period of 28 days. The initial burst release happened within 8 h of incubation and was below 10% (0.78 ± 0.1 ng). Afterward, rhBMP-2 showed a sustained release kinetic for up to 28 days of incubation and the cumulative release percentage was below 29% (2.71 ± 0.3 ng), which indicated that rhBMP-2 may be released in a sustained manner during a prolonged period (more than 28 days).

3.4. MC3T3-E1 cell proliferation

The proliferation and morphology of MC3T3-E1 cells on Ti-**6** for 1, 3 and 7 days was visually observed by fluorescence microscope, as compared to those on the control (48-well plate), Ti-**1**, **2** and **5** (Fig. 4A). Gradual increases in the cell proliferations were observed on all samples over time. In addition, the cells cultured on all samples were stretched in all directions over time. In particular, Ti-**6** showed the highest cell proliferation rate and the quickest stretching velocity in all samples. We quantitatively examined the proliferation rates of MC3T3-E1 cells cultured on all samples for 1, 3 and 7 days (Fig. 4B). The cell proliferation rates of MC3T3-E1 cultured on Ti-**2**, **5** and **6** only showed a marginal difference at day 1, as compared to that cultured on Ti-**1** as well as the control. On the other hand, the cell proliferation rates of MC3T3-E1 cultured on Ti-**5** and **6** were similar to that cultured on Ti-**1** as well as the control at 3 and 7 days of culture. Moreover, Ti-**6** showed the highest cell proliferation rate even though the cell proliferation rate was not statistically significant, as compared that of the control. But, the cell proliferation rate showed a statistical significance, as compared to that of Ti-**1**. The results indicated that Ti-**6** can be used as a good implant to enhance the cell proliferation rate of MC3T3-E1.

3.5. Level of ALP activity

We examined the ALP activity level of MC3T3-E1 cells cultured on Ti-**6** for 7, 14 and 21 days, as compared to that on the control (48-well plate), Ti-**1**, **2** and **5** (Fig. 5). Generally, ALP activity is expressed at the initial stage of bone formation (Takagishi et al., 2006), which was well in agreement with our result. Although ALP activity levels on Ti-**1**, **2**, **5** and **6** statistically showed significant differences compared to that on control, the ALP activity levels were not substantial at 7 days of culture. However, significant increases in the ALP activity levels were observed on Ti-**2**, **5** and **6** at 14 and 21 days of culture. Moreover, Ti-**6** showed the highest ALP activity level, indicating that the sample can be used as a good implant to accelerate the osteogenic differentiation of MC3T3-E1 cells.

3.6. Amount of calcium deposition

We examined the amount of calcium deposited on Ti-**6** cultured with MC3T3-E1 cells for 14 and 21 days as compared to that on the control (48-well plate), Ti-**1**, **2,** and **5** (Fig. 6). Calcium was visually found to be heavily deposited on Ti-**2**, **5** and **6** at 21 days of culture, as compared to the control and Ti-**1** (Fig. 6A). Moreover, Ti-**6** showed the largest amount of calcium deposition (Fig. 6B), indicating that the sample can be used as a good implant to accelerate the osteogenic differentiation of MC3T3-E1 cells.

3.7. Real-time PCR

The expressions of osteoblast mRNA gene markers, including OXS, Runx2, COL1, OC, OP and BSP, was examined on Ti-**2**, **5** and **6** cultured with MC3T3-E1 cell, as compared to the control (48-well plate) and Ti-**1** (Fig. 7). As osteogenic transcription factors, a gradual increase in the OXS mRNA expression was observed on all samples over time (Fig. 7A). On the other hand, Runx2 mRNA expression increased for 14 days of culture, and then decreased thereafter (Fig. 7B). Among the samples, Ti-**6** showed the highest expressions of OSX and Runx2 mRNA genes. Fig. 7C shows mRNA expression of COL1 synthesis on all samples for 21 days of culture. COL1 is generally regarded as an early marker during the proliferation of osteoblast cells (Lian, Stein, & Aubin, 2003), which is well in agreement with our results. A gradual decrease in the COL1 synthesis was observed on all samples over time. At each predetermined time point, COL1 synthesis significantly increased in the order of Ti-**1**, **2**, **5** and **6**. Fig. 7D shows the OC mRNA expression on all samples for 21 days of culture. Gradual increases and decreases in the OC and the OP mRNA expressions were observed on all samples over time (Fig. 7D and E). The mRNA genes showed increased expressions in the order of Ti-**1**, **2**, **5,** and **6**. In particular, significant increases of OC and OP mRNA expressions were observed on Ti-**6** at 14 and 21 days of culture. The mRNA expression of BSP on all samples showed a similar behavior, as compared to that of OC (Fig. 7F). Among the samples, a significant increase in the BSP mRNA expression was observed on Ti-**6**.

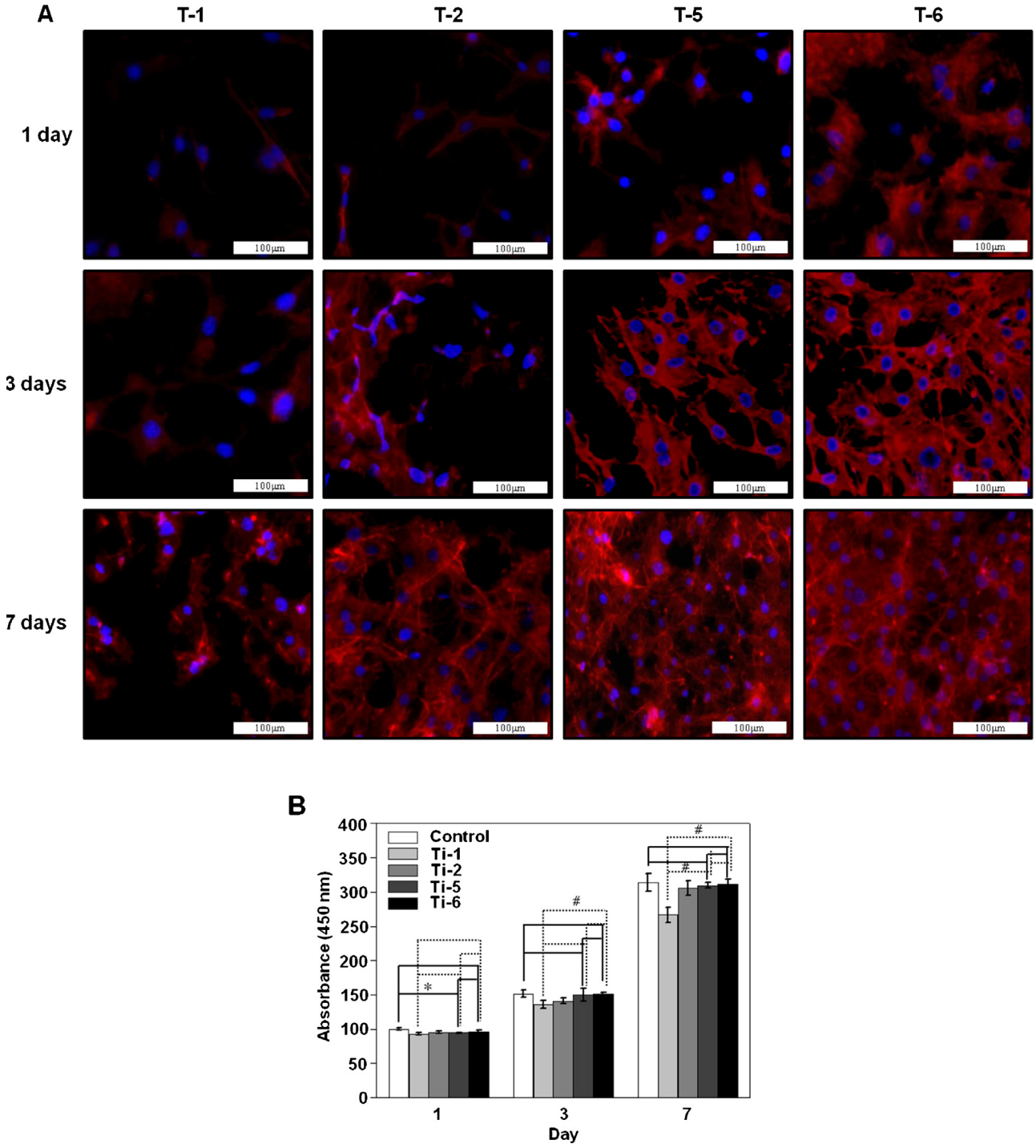

Fig. 4. Proliferation of MC3T3-E1 cells cultured on control (48-well plate), Ti-**1**–**2**, and Ti-**5**–**6** for 1, 3 and 7 days, examined by (A) fluorescence microscope and (B) CCK-8 assays.

4. Discussion

Click reaction was first introduced by Kolb et al. (2001), which is not a specific reaction but one that mimics nature. Click reaction has been used in several applications including the bioconjugation of synthetic labels to biomolecules, materials science such as synthesis of dendrimers, surface modification of single walled carbon nanotubes (SWNTs) for molecular electronics, sensors and field emission devices, engineering techniques for self assembled monolayer (SAM) formation on metal surfaces, the synthesis of rotaxanes and drug discovery (Kolb et al., 2001; Rostovtsev et al., 2002). In the present study, we modified the surface of titanium by the concept of click reaction. Pristine and surface-modified Ti-**1**–**6** were characterized by static contact angle and XPS measurements (Table 2), resulting in the successful surface modifications.

We examined the release kinetics of rhBMP-2 from Ti-**6** for 28 days of incubation (Fig. 3). Generally, BMP family comprises significant growth factors for the regeneration of bone and cartilage. Among these, rhBMP-2 has been particularly well known as a growth factor for very strong osteoinductive activity. However, BMP-2 has several problems including high cost, the need of high dose and short half-life (Sellers et al., 2010). Hence, effective

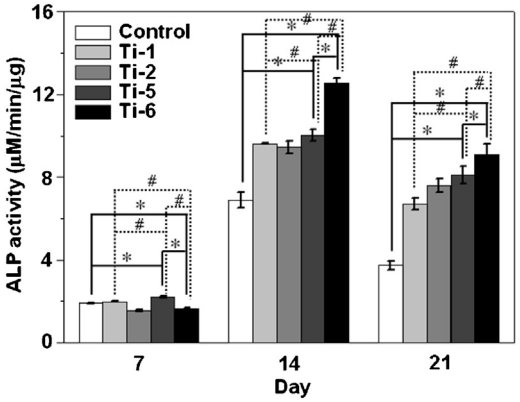

Fig. 5. ALP activity level of MC3T3-E1 cells cultured on control (48-well plate), Ti-**1**, **2**, **5** and **6** for 7, 14, and 21 days.

systems for the controlled release of rhBMP-2 have to be considered to stimulate bone regeneration. In the present study, we used heparin-binding system to release rhBMP-2 in a sustained manner because rhBMP-2 contains a strong heparin-binding site allowing good binding with heparin (Ruppert et al., 1996). We found that rhBMP-2 using heparin-based system was released for 28 days in a sustained manner.

The proliferation rate of MC3T3-E1 cell was examined on all samples, resulting that the cells cultured on Ti-**6** had the highest cell proliferation rate in all samples (Fig. 4), which may be attributed to the effect of rhBMP-2.

ALP activity and calcium deposition are early and late markers of osteoblastic cells, respectively. Enhanced ALP activity level and calcium deposition amount were observed on Ti-6, as compared to the control, Ti-**1**, **2** and **5** (Figs. 5 and 6), suggesting that rhBMP-2 accelerated new bone formation.rhBMP-2 has also known as one of the most potent stimulators of osteoblastic cell differentiation. Osteoblastic differentiation can be confirmed by the assay of bone-related mRNA gene expressions. We examined the mRNA expressions of OSX as a significant transcriptional factor involved in the differentiation step from preosteoblasts to fully functioning osteoblast and Runx2 as a significant regulator of osteoblastic differentiation (Nakashima & de Crombrugghe, 2003). A zinc finger transcriptional factor OSX acts downstream from Runx2, which is predictive of bone mass formation (Nakashima & de Crombrugghe, 2003). As shown in Fig. 7A, an increase in the OSX mRNA

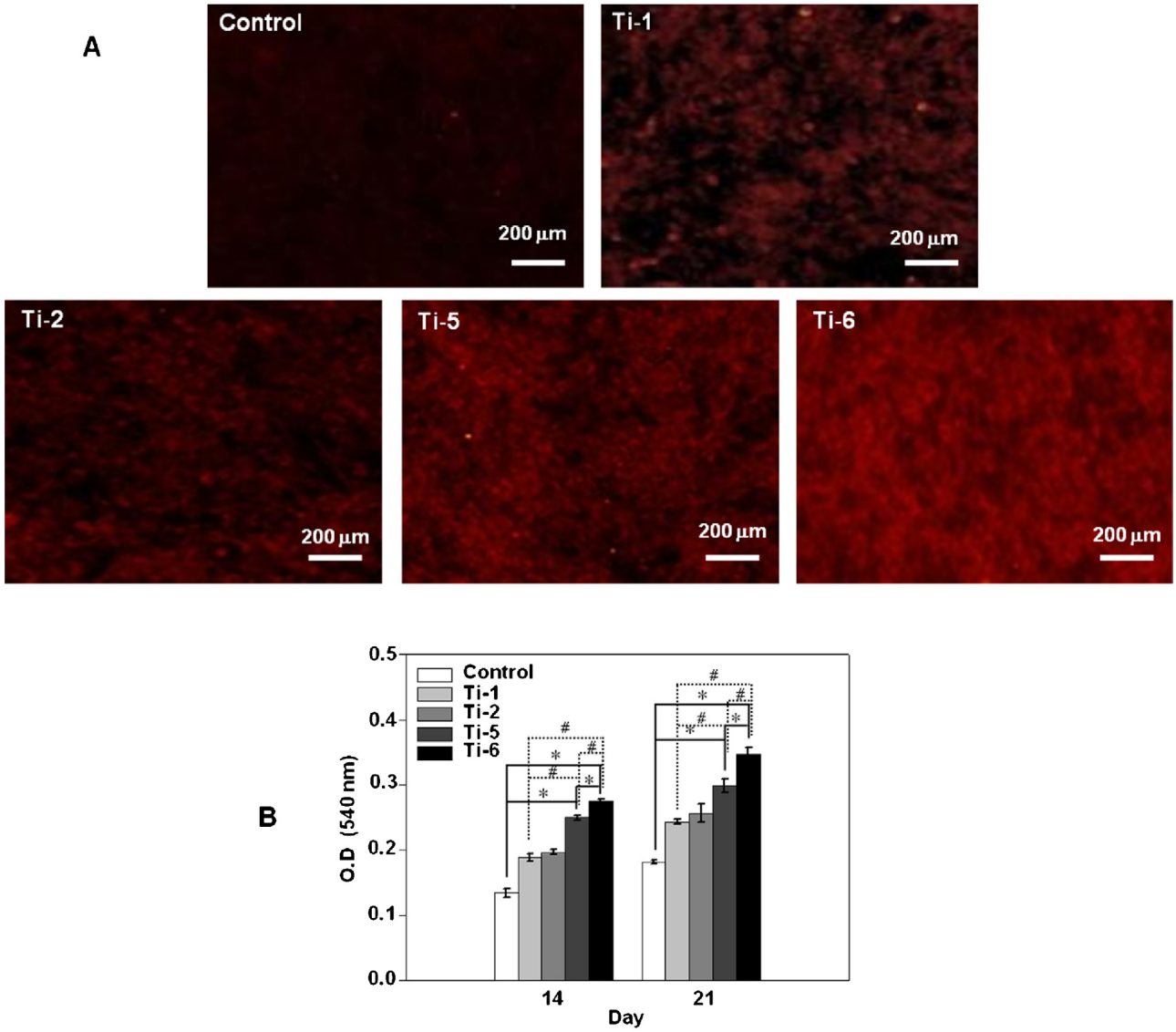

Fig. 6. (A) CLSM images of calcium deposited on control (48-well plate), Ti-**1**–**2**, **5** and **6** at 21 days of culture and (B) their quantitative calcium degree after 14 and 21 days of cultures, respectively.

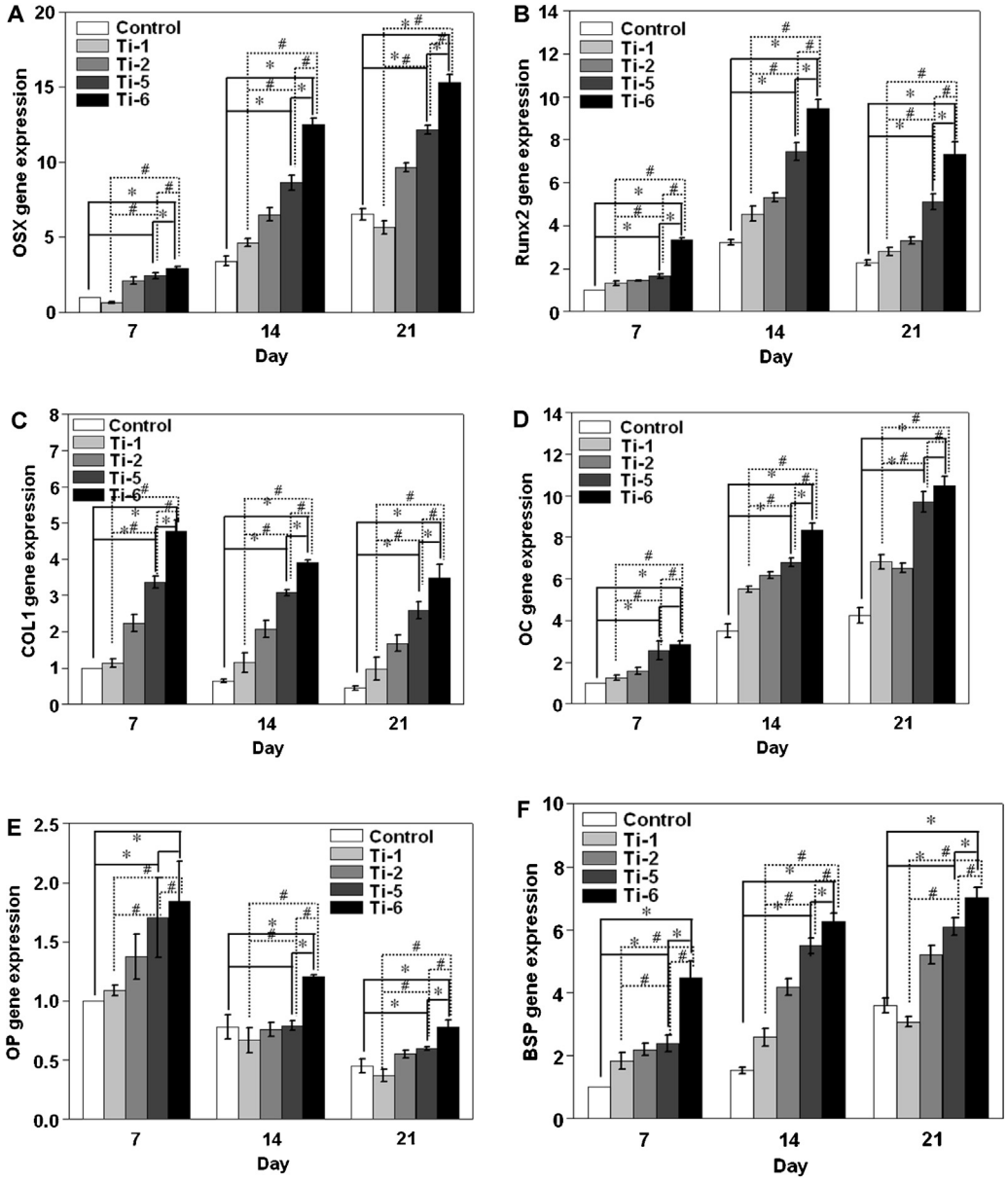

Fig. 7. Gene expressions of (A) OSX, (B) Runx2, (C) COL1, (D) OC, (E) OP and (F) BSP on control (48-well plate), Ti-**1**–**2**, **5** and **6** at 7, 14 and 21 days of cultures.

expression was observed on Ti-**6**, which may lead to the acceleration of new bone formation. Runx2 mRNA expression is induced by a Smad-dependent pathway (Nakashima & de Crombrugghe, 2003). Ti-**6** gradually showed over-expressed Runx2 mRNA expression, as compared to the control, Ti-**1**, **2** and **5** (Fig. 7B). A gradual decrease in the Runx2 mRNA expression was observed on all samples after 14 days of culture (Fig. 7B). Although Runx2 is not essential for the expression of main osteogenic mRNA genes in mature osteoblastic cells because the overexpression produces osteopenia by decreasing osteoblasts and increasing osteoclasts, the gene inhibits osteoblastic proliferation by acting on p85 PIK3 and GADD45β (Gordeladze, Reseland, Duroux-Richard, Apparailly, & Jorgensen, 2010). In the present study, we suggested that a decrease in the Runx2 mRNA expression after 14 days might accelerate osteoblasts. Also, bone is formed by complicated biological processes and controlled by expressions of the mRNA genes including COL1, ALP, OC, BSP and OP. COL1 is an early marker during the proliferation of osteoblast cells (Lamolle et al., 2009). As shown in Fig. 7C, Ti-**6** showed more significant mRNA expression of COL1, as compared to the control and Ti-**1**, mainly attributed to the effect of rhBMP-2. ALP mRNA gene expresses in the matrix maturation. In addition, OC and BSP are closely related to calcium deposition in the extracellular matrix during matrix mineralization (Lamolle et al., 2009; Stein, Lian, Stein, Van Wijnen, & Montecino, 1996). Aronow et al. (1990) have reported that OC mRNA gene harvested from the cranial bone of rat was more expressed later than ALP. Among all samples, the highest level of ALP activity and expression of OC mRNA gene were observed on Ti-**6**, mainly attributed to the effect of rhBMP-2. Unlike OC mRNA gene, OP mRNA gene expresses in the initial stage of osteoblastic differentiation and matrix mineralization (Owen et al., 1990). However, the result of Fig. 7E was different from the above-mentioned fact, which may be due to the influences of the culture condition and media. BSP is generally a late marker expressed during matrix mineralization. Ti-**6** showed the highest expression of BSP mRNA gene over time. Consequently, BMP-2 immobilized on titanium surface may induce the enhanced osteogenic differentiation of MC3T3-E1 cells.

5. Conclusions

We designed and prepared surface-propargylated Ti-**3** via click reaction and rhBMP-2-immobilized Ti-**6** to evaluate the osteogenic differentiation of MC3T3-E1 cells. The surfaces of Ti-**1**–**6** were characterized by SEM, XPS and contact angle measurements, resulting in the successful surface modifications. Ti-**3** was found to be used as a good intermediate tool to immobilize heparin. BMP-2 from Ti-**6** was released for 28 days in a sustained manner. Ti-**6** showed the highest cell proliferation rate and bone-related mRNA gene expression including OSX, Runx2, COL1, OC, OP and BSP. It is concluded that Ti-**6** can be used as a good implant to enhance bone formation.

Acknowledgments

This work was supported by grants from the Kyung Hee University in 2012 (KHU-20121678) and the National Research Foundation of Korea (NRF) Grant funded by the Korean Government (MSIP) (no. 2012R1A5A2051384).

References

Andreazza, P., De Barros, M. I., Andreazza-Vignolle, C., Rats, D., & Vandenbulcke, L. (1998). In-depth structural X-ray investigation of PECVD grown diamond films on titanium alloys. *Thin Solid Films*, *319*(1–2), 62–66.

Aronow, M. A., Gerstenfeld, L. C., Owen, T. A., Tassinari, M. S., Stein, G. S., & Lian, J. B. (1990). Factors that promote progressive development of the osteoblast phenotype in cultured fetal rat calvaria cells. *Journal of Cellular Physiology*, *143*(2), 213–221.

Buser, D., Nydegger, T., Oxland, T., Cochran, D. L., Schenk, R. K., Hirt, H. P., et al. (1999). Influence of surface characteristics on the interface shear strength between titanium implants and bone. A biomechanical study in the maxilla of miniature pigs. *Journal of Biomedical Materials Research*, *45*, 75–83.

Domenichini, B., Perriat, P., Merie, J., Basset, K., Guigue-Millot, N., & Bourgeois, S. (1999). Dynamic segregation phenomena during oxidation of titanium ferrites. *Journal of Materials Chemistry*, *9*, 1179–1183.

Gordeladze, J. O., Reseland, J. E., Duroux-Richard, I., Apparailly, F., & Jorgensen, C. (2010). From stem cells to bone: Phenotype acquisition, stabilization, and tissue engineering in animal models. *ILAR Journal*, *51*, 42–61.

Hua, Z. L., Shi, J. L., Zhang, L. X., Ruan, M. L., & Zhao, X. G. (2001). Acid-prepared mesostructures modified with TiO_2 by a template-titanium tetrabutoxide displacement. *Journal of Materials Chemistry*, *11*, 3130–3134.

Kapoor, M. P., Bhaumik, A., Inagaki, S., Kuraoka, K., & Yazawa, T. (2002). Titanium containing inorganic–organic hybrid mesoporous materials with exceptional activity in epoxidation of alkenes using hydrogen peroxide. *Journal of Materials Chemistry*, *12*, 3078–3083.

Kim, S. E., Song, S. H., Yun, Y. P., Choi, B. J., Kwon, I. L., Bae, M. S., et al. (2011). The effect of immobilization of heparin and bone morphogenic protein-2 (BMP-2) to titanium surfaces on inflammation and osteoblast function. *Biomaterials*, *32*(2), 366–373.

Kolb, H. C., Finn, M. G., & Sharpless, K. B. (2001). Click chemistry: Diverse chemical function from a few good reaction. *Angewandte Chemie International Edition*, *40*(11), 2004–2021.

Lamolle, S. F., Monjo, M., Rubert, M., Haugen, H. J., Lynqstadaas, S. P., & Ellingsen, J. E. (2009). The effect of hydrofluoric acid treatment of titanium surface on nanostructural and chemical changes and the growth of MC3T3-E1 cells. *Biomaterials*, *30*(5), 736–742.

Lian, J. B., Stein, G. S., & Aubin, J. E. (2003). Bone formation: Maturation and functional activities of osteoblast lineage cells. In M. J. Favus (Ed.), *Primers on the metabolic bone diseases and disorders of mineral metabolism* (pp. 13–28). Washington, DC: American Society for Bone and Mineral Research.

Liu, X., Chu, P. K., & Ding, C. (2004). Surface modification of titanium, titanium alloys, and related materials for biomedical applications. *Materials Science and Engineering: R*, *47*, 49–121.

Lee, B. H., Kim, J. K., Kim, Y. D., Choi, K., & Lee, J. H. (2004). In vivo behavior and mechanical stability of surface-modified titanium implants by plasma spray coating and chemical treatments. *Journal of Biomedical Materials Research Part A*, *69*(2), 279–285.

Mager, M. D., LaPointe, V., & Stevens, M. M. (2011). Exploring and exploiting chemistry at the cell surface. *Nature Chemistry*, *3*, 582–589.

Mundy, G., Garrett, R., Harris, S., Chan, J., Chen, D., Rossini, G., et al. (1999). Stimulation of bone formation in vitro and in rodents by statins. *Science*, *286*, 1946–1949.

Nakashima, K., & de Crombrugghe, B. (2003). Transcriptional mechanisms in osteoblast differentiation and bone formation. *Trends in Genetics*, *19*(8), 458–466.

Owen, T. A., Aronow, M., Shalhoub, V., Barone, L. M., Wilming, L., Tassinari, M. S., et al. (1990). Progressive development of the rat osteoblast phenotype in vitro: Reciprocal relationships in expression of genes associated with osteoblast proliferation and differentiation during formation of the bone extracellular matrix. *Journal of Cellular Physiology*, *143*(3), 420–430.

Prime, K. L., & Whitesides, G. M. (1991). Self-assembled organic monolayers: Model systems for studying adsorption of proteins at surfaces. *Science*, *24*, 1164–1167.

Rostovtsev, V. V., Green, L. G., Fokin, V. V., & Sharpless, K. B. (2002). A stepwise huisgen cycloaddition process: Copper(I)-catalyzed regioselective ligation of azides and terminal alkynes. *Angewandte Chemie International Edition*, *41*, 2596–2599.

Ruppert, R., Hoffmann, E., & Sebald, W. (1996). Human bone morphogenetic protein 2 contains a heparin-binding site which modifies its biological activity. *European Journal of Biochemistry*, *237*, 295–302.

Sellers, R. S., Zhang, R., Glasson, S. S., Kim, H. D., Peluso, D., & D'Augusta, D. A. (2010). Repair of articular cartilage defects on year after treatment with recombinant human bone morphogenetic protein-2 (rhBMP-2). *Journal of Bone and Joint Surgery*, *82*, 151–160.

Shimasaki, S., Zachow, R. J., Li, D., Kim, H., Iemura, S., Ueno, N., et al. (1999). A functional bone morphogenetic protein system in the ovary. *Proceedings of the National Academy of Sciences of the United States of America*, *96*(13), 7282–7287.

Stein, G. S., Lian, J. B., Stein, J. L., Van Wijnen, A. J., & Montecino, M. (1996). Transcriptional control of osteoblast growth and differentiation. *Physiological Reviews*, *76*(2), 593–629.

Sutherland, D. S., Forshaw, P. D., Allen, G. C., Brown, I. T., & Williams, K. R. (1993). Surface analysis of titanium implants. *Biomaterials*, *14*, 893–899.

Takagishi, Y., Kawakami, T., Hara, Y., Shinkai, M., Takezawa, T., & Nagamune, T. (2006). Bone-like tissue formation by three-dimensional culture of MG63 osteosarcoma cells in gelatin hydrogels using calcium-enriched medium. *Tissue Engineering*, *12*, 927–937.

van Dijk, M., Rijkers, D. T. S., Liskamp, R. M. J., van Nostrum, C. F., & Hennink, W. E. (2009). Synthesis and applications of biomedical and pharmaceutical polymers via click chemistry methodologies. *Bioconjugate Chemistry*, *20*(11), 2001–2016.

Wennerberg, A., Albrektsson, T., Johansson, C. B., & Andersson, B. (1996). An experimental study of turned and grit blasted screw-shaped implants with special emphasis on effects of blasting material and surface topography. *Biomaterials*, *17*, 15–22.

Xiao, S. J., Textor, M., & Spencer, N. D. (1998). Covalent attachment of cell-adhesive, (Arg-Gly-Asp)-containing peptides to titanium surfaces. *Langmuir*, *14*(19), 5507–5516.

Xue, W., Deng, Z., Lai, Y., & Chen, R. (1998). Analysis of phase distribution for ceramic coatings formed by microarc oxidation on aluminum alloy. *Journal of the American Ceramic Society*, *81*(5), 1365–1368.